AGU PUBLICATIONS

JGR

Journal of Geophysical Research: Atmospheres

RESEARCH ARTICLE
10.1002/2016JD025156

Key Points:
- Isoprene-OA formation is rapid via the IEPOX reactive uptake downwind of power plant plumes
- Sulfate enhances isoprene-OA formation due to both enhanced particle surface area and particle acidity
- About 25% of the OA reduction in the southeastern United States could arise from the sulfate control over isoprene-OA formation

Supporting Information:
- Supporting Information S1

Correspondence to:
N. L. Ng,
ng@chbe.gatech.edu

Citation:
Xu, L., et al. (2016), Enhanced formation of isoprene-derived organic aerosol in sulfur-rich power plant plumes during Southeast Nexus, *J. Geophys. Res. Atmos.*, *121*, 11,137–11,153, doi:10.1002/2016JD025156.

Received 28 MAR 2016
Accepted 13 AUG 2016
Accepted article online 4 SEP 2016
Published online 29 SEP 2016

Enhanced formation of isoprene-derived organic aerosol in sulfur-rich power plant plumes during Southeast Nexus

Lu Xu[1], Ann M. Middlebrook[2], Jin Liao[2,3,4,5], Joost A. de Gouw[3,6], Hongyu Guo[7], Rodney J. Weber[7], Athanasios Nenes[1,7,8,9], Felipe D. Lopez-Hilfiker[10], Ben H. Lee[10], Joel A. Thornton[10], Charles A. Brock[2], J. Andrew Neuman[2,3], John B. Nowak[2,3,11], Ilana B. Pollack[2,3,12], Andre Welti[3,13], Martin Graus[2,3,14], Carsten Warneke[2,3], and Nga Lee Ng[1,7]

[1]School of Chemical and Biomolecular Engineering, Georgia Institute of Technology, Atlanta, Georgia, USA, [2]Chemical Sciences Division, NOAA Earth System Research Laboratory, Boulder, Colorado, USA, [3]Cooperative Institute for Research in Environmental Sciences, University of Colorado Boulder, Boulder, Colorado, USA, [4]Now at Atmospheric Chemistry and Dynamics Laboratory, NASA Goddard Space Flight Center, Greenbelt, Maryland, USA, [5]Now at Universities Space Research Association, Columbia, Maryland, USA, [6]Department of Chemistry and Biochemistry, University of Colorado Boulder, Boulder, Colorado, USA, [7]School of Earth and Atmospheric Sciences, Georgia Institute of Technology, Atlanta, Georgia, USA, [8]Institute of Chemical Engineering Sciences (ICE-HT), Foundation for Research, Patras, Greece, [9]Institute for Environmental Research and Sustainable Development, National Observatory of Athens, Palea Penteli, Greece, [10]Department of Atmospheric Sciences, University of Washington, Seattle, Washington, USA, [11]Now at Aerodyne Research Inc., Billerica, Massachusetts, USA, [12]Now at Department of Atmospheric Science, Colorado State University, Fort Collins, Colorado, USA, [13]Now at Department of Physics, Leibniz Institute for Tropospheric Research, Leipzig, Germany, [14]Now at Institute of Meteorology and Geophysics, University of Innsbruck, Innsbruck, Austria

Abstract We investigate the effects of anthropogenic sulfate on secondary organic aerosol (SOA) formation from biogenic isoprene through airborne measurements in the southeastern United States as part of the Southeast Nexus (SENEX) field campaign. In a flight over Georgia, organic aerosol (OA) is enhanced downwind of the Harllee Branch power plant but not the Scherer power plant. We find that the OA enhancement is likely caused by the rapid reactive uptake of isoprene epoxydiols (IEPOX) in the sulfate-rich plume of Harllee Branch, which was emitting at least 3 times more sulfur dioxide (SO_2) than Scherer, and more aerosol sulfate was produced downwind. The contrast in the evolution of isoprene-derived OA concentration between two power plants with different SO_2 emissions provides an opportunity to investigate the magnitude and mechanisms of particle sulfate on isoprene-derived OA formation. We estimate that 1 $\mu g\ sm^{-3}$ reduction of sulfate would decrease the isoprene-derived OA by $0.23 \pm 0.08\ \mu g\ sm^{-3}$. Based on a parameterization of the IEPOX heterogeneous reactions, we find that the effects of sulfate on isoprene-derived OA formation in the power plant plume arises from enhanced particle surface area and particle acidity, which increases both IEPOX uptake to particles and subsequent aqueous-phase reactions, respectively. The observed relationships between isoprene-OA, sulfate, particle pH, and particle water in previous field studies are explained using these findings.

1. Introduction

Secondary organic aerosol (SOA), which is formed in the atmosphere via the oxidation of volatile organic compounds (VOCs), accounts for a large fraction of submicron particulate matter globally [*Hallquist et al.*, 2009; *Jimenez et al.*, 2009]. In the southeastern United States, a large fraction of SOA originates from biogenic VOCs in summer [*Liao et al.*, 2007; *Spracklen et al.*, 2011; *Weber et al.*, 2007; *Xu et al.*, 2015a; *Xu et al.*, 2015b]. However, the SOA formation process is largely mediated by anthropogenic pollutants, such as nitrogen oxides (NO_x) and aerosol sulfate [*Carlton et al.*, 2010; *Hoyle et al.*, 2011; *Xu et al.*, 2015a; *Xu et al.*, 2015b]. Long-term measurements (1999–2013) at the Southeastern Aerosol Research and Characterization (SEARCH) network have revealed a significant decreasing trend in ambient concentrations of sulfur dioxide (SO_2) and NO_x, which is caused by regulations of anthropogenic emissions from power plants and vehicles [*Hidy et al.*, 2014], as well as the switch from coal to natural gas in many power plants [*de Gouw et al.*, 2014]. Meanwhile, the concentration of organic carbon (OC) has also decreased significantly in the same region as shown in *Hidy et al.* [2014]. However, the causes for the OC reduction were less clear.

Blanchard et al. [2015] estimated that about 45% of OC in the southeastern United States derives from combustion sources (vehicles and biomass burning), which contributes the most to the OC reduction. In addition to the reduction in primary OC from combustion sources, secondary OC from biogenic VOCs also likely decreases, due to the reduction in NO_x and SO_2 and their interactions with biogenic emissions. For example, *Blanchard et al*. [2015] observed an association between OC and sulfate based on a statistical analysis of the long-term SEARCH data. The amount of sulfate-associated OC accounted for ~25% of average OC concentration from 1999 to 2013. Also, as shown in *Xu et al*. [2015a], the correlation between OC and sulfate in the SEARCH data is substantially better in summer than in winter.

One possible explanation for the association between OC and sulfate arises from the effect of sulfate on biogenic SOA formation, especially isoprene. Globally, isoprene is the single largest contributing compound to VOC emissions from vegetation [*Guenther et al*., 2012]. In the southeastern United States, isoprene is the most abundant biogenic VOC [*Goldstein et al*., 2009; *Guenther et al*., 2012]. Laboratory studies have revealed that the isoprene SOA yield is greatly enhanced in the presence of acidic sulfate seed particles [*Edney et al*., 2005; *Kleindienst et al*., 2006; *Liu et al*., 2015; *Surratt et al*., 2007; *Surratt et al*., 2010]. The enhancement is due to the reactive uptake of isoprene epoxydiols (IEPOX) [*Gaston et al*., 2014; *Lin et al*., 2012; *Riedel et al*., 2015; *Surratt et al*., 2010; *Wang et al*., 2005]. IEPOX are isoprene oxidation products from the peroxy radical (RO_2) + hydroperoxyl radical (HO_2) pathway [*Paulot et al*., 2009b]. Positive matrix factorization (PMF) analysis of aerosol mass spectrometry data has resolved an isoprene-derived organic aerosol factor (i.e., isoprene-OA) at multiple sampling sites [*Budisulistiorini et al*., 2016; *Budisulistiorini et al*., 2013; *Chen et al*., 2015; *Hu et al*., 2015; *Robinson et al*., 2011; *Slowik et al*., 2011; *Xu et al*., 2015a; *Xu et al*., 2015b]. This factor has been interpreted as a surrogate for isoprene SOA through IEPOX reactive uptake. Specifically, PMF analysis of high-resolution aerosol mass spectrometer (AMS) data showed that isoprene-OA accounted for 18–36% of OA in summer in the southeastern United States [*Xu et al*., 2015a; *Xu et al*., 2015b].

Based on measurements at multiple sites in the southeastern United States, *Xu et al*. [2015b] showed that isoprene-OA is strongly associated with sulfate but not associated with particle pH or particle water as suggested by prior laboratory studies. This strong correlation between isoprene-OA and sulfate has been repeatedly observed in many studies [*Budisulistiorini et al*., 2015; *Hu et al*., 2015] and reproduced in chemical transport models [*Marais et al*., 2015; *McNeill*, 2015; *McNeill et al*., 2012; *Pye et al*., 2013]. However, a coherent explanation regarding the relationships between isoprene-OA and sulfate, particle pH, and particle water has not emerged. The model results by *Marais et al*. [2015] suggest that the correlation between isoprene-OA and sulfate is caused by sulfate's influence on volume and pH, although the role of particle volume is not explicitly discussed and remains unclear. Regarding the repeatedly observed lack of correlation between isoprene-OA and particle pH in ambient measurements [*Budisulistiorini et al*., 2015; *Xu et al*., 2015b], some studies suggested that it is because isoprene-OA measured at a surface site is affected by transport, during which the particle pH can change [*Budisulistiorini et al*., 2013]. However, *Budisulistiorini et al*. [2015] modeled the concentration of IEPOX-derived SOA tracers with good accuracy by using local particle pH and particle water at Look Rock, TN, even though the observed isoprene SOA did not correlate with local particle pH. In addition, in *Xu et al*. [2015b], where isoprene-OA was largely locally produced at Centreville, AL, as indicated by the highly reproducible diurnal variation of isoprene-OA regardless of the origin of air masses, isoprene-OA is still not correlated with particle pH. Thus, transport may not explain the lack of correlation between isoprene-OA and particle pH. Other possible mechanisms of sulfate influence on isoprene-OA formation are through the surface accommodation process [*Lin et al*., 2013] or nucleophilic effects of sulfate [*Xu et al*., 2015b].

In this study, we investigate the mechanisms and kinetics of anthropogenic emissions on isoprene SOA formation based on airborne measurements in the southeastern United States, a region with large emissions from both anthropogenic and biogenic sources. We sampled downwind from power plants in Georgia. The power plant studies serve as a unique perturbation experiment in the atmosphere by injecting anthropogenic emissions (NO_x and SO_2) into isoprene-rich air masses. We use measurements made downwind from two power plants with differing SO_2 emissions, which provides an opportunity to examine the sensitivity of isoprene SOA to varying amounts of particle sulfate in otherwise nearly identical ambient conditions.

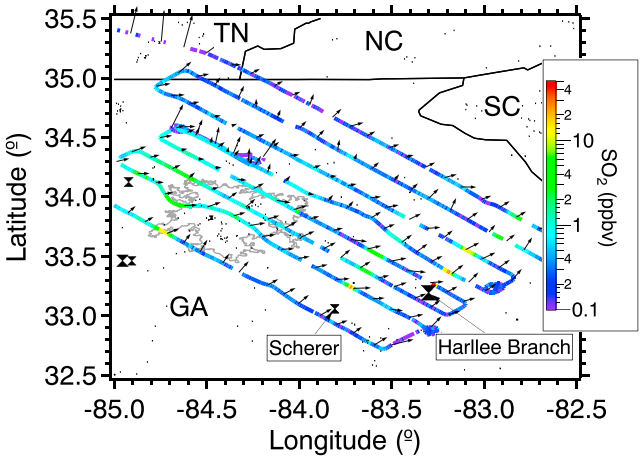

Figure 1. Flight track of the NOAA WP-3D aircraft presented in this study. The flight track is colored by SO_2 concentration. The direction of arrow represents wind direction, and the length of arrow is proportional to wind speed. The power plants are marked in the figure and sized by its SO_2 emission. The two power plants of interest to this study, Scherer and Harllee Branch, are labeled in the figure. The gray circled region represents urban Atlanta.

2. Measurements and Models

Measurements were performed as part of the Southeast Nexus (SENEX) campaign in June and July 2013 [*Warneke et al.*, 2016]. In the SENEX campaign, the NOAA WP-3D aircraft flew 20 research flights over the southeastern United States. In the current study, we focused on the flight on 16 June 2013, when the aircraft flew over Georgia. The flight track is shown in Figure 1. We focus our analysis on the measurements at different downwind distances of two power plants, Scherer and Harllee Branch, the locations of which are shown in Figure 1. Both Scherer and Harllee Branch are coal-fired power plants, but they have different emissions of NO_x and SO_2. As shown in Figure S1, the daytime NO_x and SO_2 emissions of Scherer are only about one third and one sixth of those of Harllee Branch, respectively, which is a result of the installation of different emissions reduction equipment in Scherer compared to Harllee Branch according to Continuous Emissions Monitoring System (http://www3.epa.gov/ttn/emc/cem.html). The wind direction for this flight was constantly from the southwest, resulting in a well-defined plume of emissions that was advected to the northeast. We note that there was a biomass burning source located upwind of the two power plants, and the plume from this source advected between the power plants. As will be discussed below, portions of this plume mixed with the Scherer plume in some transects. The gas phase chemistry in these plumes is described in a parallel paper that focuses on the effect of NO_x on oxidation rates and the formation of isoprene products such as formaldehyde [*de Gouw et al.*, 2015].

A suite of instruments were deployed aboard the aircraft. The instruments of interest to our study are summarized in Table S1 and discussed briefly below. A compact time-of-flight aerosol mass spectrometer (cToF-AMS) was deployed to measure the composition of nonrefractory submicron particles [*Bahreini et al.*, 2008; *Bahreini et al.*, 2009; *Canagaratna et al.*, 2007]. PMF analysis was performed on the organic mass spectra of the whole flight for OA source apportionment (supporting information). The collection efficiency (CE) for the AMS data was determined according to the composition-dependent algorithm proposed by *Middlebrook et al.* [2012] (Figure S2a). We validated the application of composition-dependent CE by converting the mass concentrations of nonrefractory species (measured by AMS) and refractory black carbon (measured by single-particle soot photometer) to volume concentration (denoted as composition-based volume) (supporting information). Then we compared the composition-based volume with Ultra-High Sensitivity Aerosol Size spectrometer (UHSAS) measurements, which reports the particle size distribution in the range of 70–1000 nm [*Brock et al.*, 2016]. As shown in Figure S2b, the composition-based volume for this flight agrees well with the UHSAS volume (slope = 1.01 ± 0.06). Even in the plume where the particle composition changes largely and there is an increase in smaller-sized particles, they still show excellent agreement (slope = 0.97 ± 0.04). Depending on the organic aerosol density, the accuracy of the composition-based volume relative to the UHSAS volume for this flight is ±16% (Figure S2c). All of the submicron aerosol instrumentation sampled air from behind a low turbulence inlet and a 1 μm aerodynamic diameter impactor [*Brock et al.*, 2016; *Wagner et al.*, 2015]. The air in this aerosol sampling line was passively dried by ram heating, and the warmer temperature inside the aircraft compared to ambient. For the flight on 16 June 2013 analyzed in this study, the mean ambient relative humidity (RH) was 68%, and the mean RH downstream of the AMS sampling inlet was 36%. The air entering the UHSAS was further dried to about 15% RH with a Nafion dryer.

A high-resolution time-of-flight chemical ionization mass spectrometer (HR-CIMS) using iodide adducts was deployed to measure a suite of oxygenated volatile organic compounds (oVOCs) at high frequency (1 Hz). Detailed working principles and sampling protocol can be found in *Lee et al*. [2014]. The instrument is able to elucidate the chemical composition of hundreds of molecular ions from the high mass accuracy and resolution, but it does not provide structural information nor isomer separation. Among all the oVOCs detected by the CIMS, the signal for $C_5H_{10}O_3$ species which has contribution from two isomers, isoprene hydroxyhydroperoxides (ISOPOOH) and isoprene epoxydiols (IEPOX), is of interest to our study.

The particle liquid water content (H_2O_{ptcl}) was calculated based on water uptake by both organics and inorganics [*Guo et al*., 2015] and the measured ambient meteorological data [*Warneke et al*., 2016]. The H_2O_{ptcl} uptake by organics was calculated based on the organic concentration (measured by AMS) and hygroscopicity (i.e., κ_{org}) [*Petters and Kreidenweis*, 2007]. Considering uncertainties in κ_{org} from previous measurements under different saturation states [*Brock et al*., 2016; *Cerully et al*., 2015], we performed sensitivity tests by varying κ_{org} from 0 to 0.2, which has negligible effects on the conclusions (Figure S3). An average value of 0.1 was selected for κ_{org}. The particle-phase H^+ and H_2O_{ptcl} uptake by inorganics were predicted using the thermodynamic model ISORROPIA II [*Fountoukis and Nenes*, 2007]. In addition to the particle-phase inorganic ions (i.e., sulfate, nitrate, ammonium, and chloride measured by AMS), gas phase HNO_3 and NH_3 measured from the aircraft were also included in the model prediction of H^+ and pH [*Hennigan et al*., 2015]. The particle-phase pH was calculated by

$$\mathrm{pH} = -\log_{10} a_{\mathrm{H}}^{+} = -\log_{10}\left(\frac{\mathrm{H}^{+}}{\mathrm{LMass}} \times \rho_{\mathrm{particle}} \times 1000\right) \quad (1)$$

where H^+ and LMass are the mass concentrations of particle hydronium ion and total aqueous-phase output from ISORROPIA II ($\mu g\, sm^{-3}$), $\rho_{particle}$ is the particle density ($g\, cm^{-3}$), and a_{H}^{+} is the H^+ activity in the aqueous phase ($mol\, L^{-1}$). The modeled HNO_3, NH_3, and particle NH_4^+ agree within 20% of the measurements (Figure S4), which supports the accuracy of our pH calculation. The details about the calculation of particle water and particle acidity are discussed in the supporting information.

3. Results and Discussion

3.1. Evolution of Species Downwind of the Power Plants

Plumes from the two power plants, Scherer and Harllee Branch, were each intercepted five times at different downwind distances, which allows us to investigate the evolution of plume composition, with a focus on organic aerosol. In order to compare the species concentration inside and outside the plume, for each intercept, we calculate the average plume concentration of a certain species based on 1 min measurements in the center of the plume (defined by peak NO_2 concentration) and we calculate the average concentration outside the plume based on 2 min measurements before and after the plume intercepts (see Figure S5 for details). Figure 2 shows the evolution of species of interest, and Figure S6 shows the evolution of auxiliary species. While the SO_2 concentration is enhanced in both plumes compared to outside the plume (Figure 2a), the enhancement magnitude is larger in the Harllee Branch plume due to larger emissions of SO_2. The oxidation of SO_2 causes the enhancement of sulfate downwind of the power plants (Figure 2b). Figure 2c shows that enhancements in OA are observed at all intercepts of the Harllee Branch plume. The largest enhancement occurred at the fourth intercept (i.e., 62.8 km downwind of Harllee Branch), where the OA increased by as much as $1.8\, \mu g\, sm^{-3}$ after correcting for the particle collection efficiency in AMS. In contrast, the OA was only enhanced for the first two intercepts of Scherer plume. Below, we address the causes for OA enhancement in both plumes, with a focus on the Harllee Branch plume.

3.2. Reasons for OA Enhancement in the Plumes

The OA enhancement for the first two intercepts of Scherer plume is likely caused by a biomass burning plume that partly merged with the Scherer plume. Black carbon (Figure S7) and other tracers for biomass burning (e.g., CO and acetonitrile) are enhanced in the first two intercepts of Scherer plume. This biomass burning plume has negligible influence on the Harllee Branch as neither black carbon nor acetonitrile is enhanced in the Harllee Branch plume.

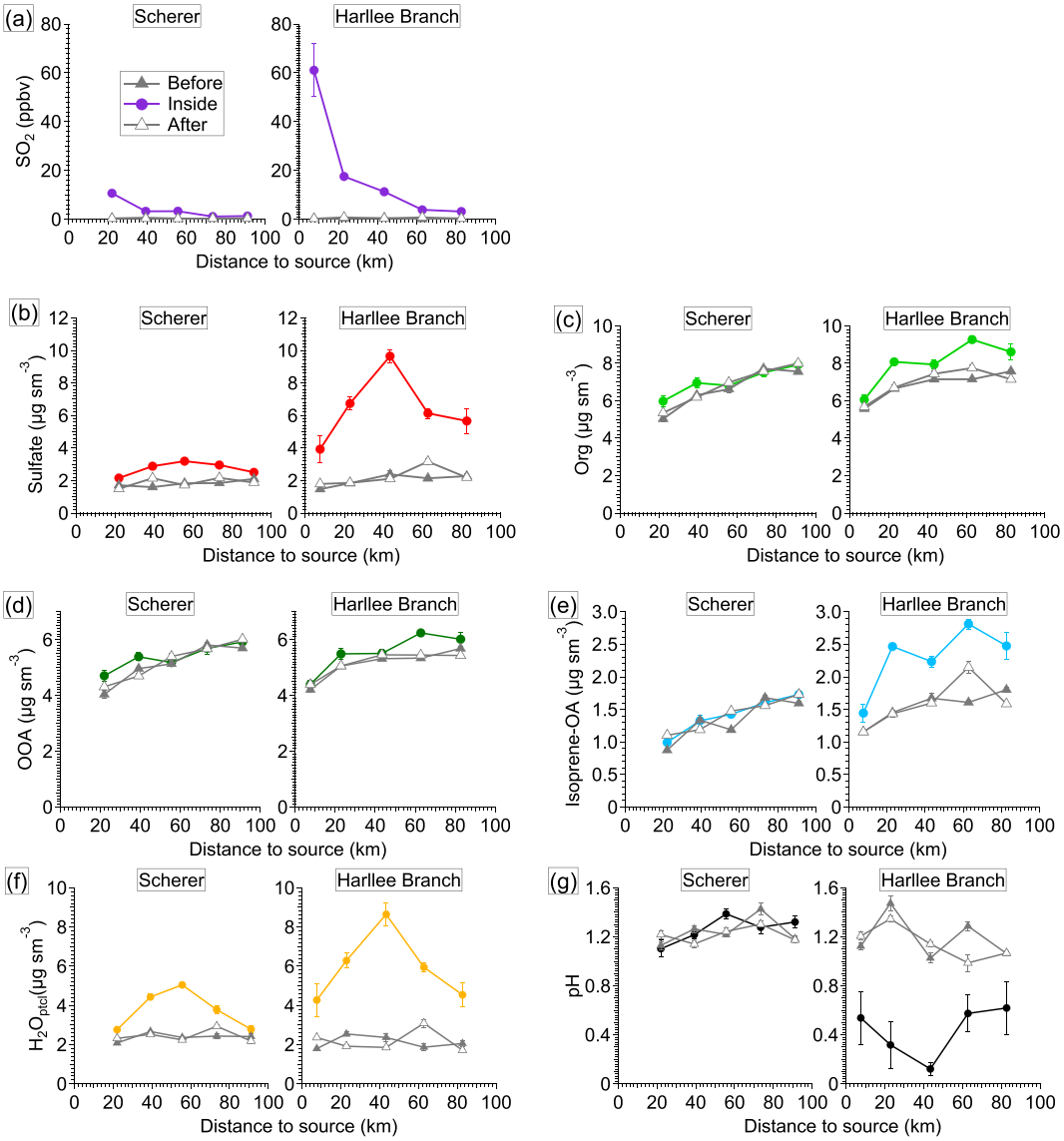

Figure 2. Evolution of (a) SO_2, (b) sulfate, (c) organics, (d) oxygenated organic aerosol (OOA), (e) isoprene-derived organic aerosol (isoprene-OA), (f) particle water, and (g) particle pH. The error bars represent the standard error. The error bars of some data points are smaller than the symbol size of the data points. Details about the particle water and pH calculation can be found in the supporting information. The sulfate concentration reported here is measured by AMS, which includes both SO_4^{2-} and HSO_4^-. The ISORROPIA calculated concentrations of SO_4^{2-} and HSO_4^- are shown in Figure S10.

To examine the reasons for the OA enhancement in the Harllee Branch plume, we first investigate the composition of OA formed in the plume. For each intercept, we subtract the OA mass spectra outside the plume from the OA mass spectra inside the plume and then normalize the difference mass spectra to the total difference signal. As shown in Figure 3, the composition of OA formed in the Harllee Branch is distinctly different from that outside the plume. Outside the plume, the most prominent signal is *m/z* 44 (mainly CO_2^+, a tracer for carboxylic acids [*Canagaratna et al.*, 2015; *Ng et al.*, 2010]). Inside the Harllee Branch plumes, we note a substantial signal at *m/z* 53 and *m/z* 82, which are attributed to isoprene SOA via the reactive uptake of IEPOX [*Allan et al.*, 2014; *Budisulistiorini et al.*, 2013; *Lin et al.*, 2012; *Liu et al.*, 2015; *Robinson et al.*, 2011; *Xu et al.*, 2015a; *Xu et al.*, 2015b]. The ion *m/z* 82 accounts for about 2.1–3.5% of the OA formed in the Harllee Branch plume. The enhancement of *m/z* 82 suggests that the formation of isoprene SOA contributes to the OA enhancement in the Harllee Branch plume. Although the cToF-AMS used in this study cannot separate the ions at *m/z* 82 ($^{34}SO_3^+$, $C_4H_2O_2^+$, $C_5H_6O^+$, and $C_6H_{10}^+$), the mass resolution is sufficient to

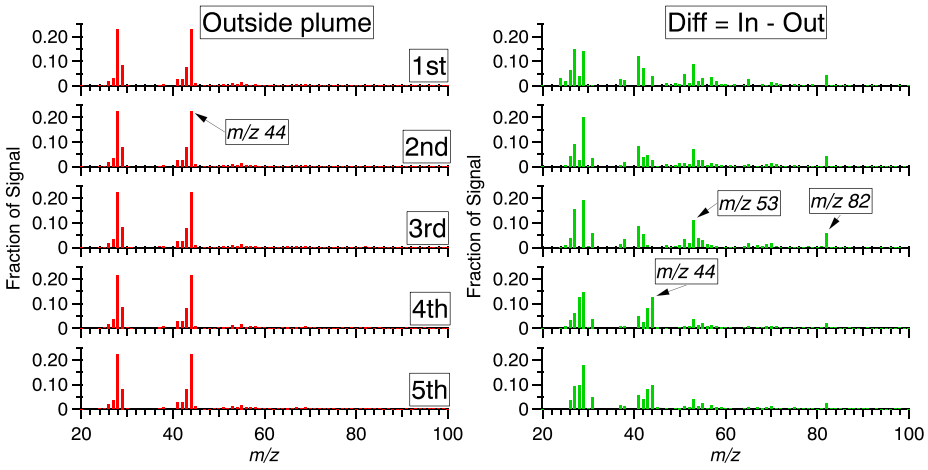

Figure 3. (left column) Normalized mass spectra of OA outside the Harllee Branch plume. (right column) Normalized mass spectra of OA formed inside the Harllee Branch plume, which are calculated by subtracting the OA mass spectra outside the plume from that inside the plume and then normalizing the difference mass spectra to the total difference signal.

indicate that the signal at *m/z* 82 is distinctly not solely due to $^{34}SO_3^+$ or $C_6H_{10}^+$ (Figure S8). It is likely dominated by $C_5H_6O^+$ based on high-resolution AMS data obtained in surface measurements in the southeastern United States [*Xu et al*., 2015a; *Xu et al*., 2015b].

To further investigate the reasons for OA enhancement in the plumes, we perform PMF analysis on organic mass spectra for source apportionment. Two OA factors, oxygenated OA (OOA) and isoprene-derived OA (isoprene-OA), are resolved for this flight. The mass spectra and time series of these two factors are shown in Figure 4. The mass spectrum of OOA is characterized by high f_{44} (ratio of *m/z* 44 to total OA signal), which indicates that this factor is highly oxidized [*Ng et al*., 2010]. For the entire flight on 16 June, OOA accounts for 76% of OA on average. The time series of OOA correlates well with CO ($R = 0.92$, Figure 4b), which is consistent with previous field studies [*Bahreini et al*., 2009; *Sullivan et al*., 2006; *Weber et al*., 2007; *Worton et al*., 2011].

The mass spectrum of the isoprene-OA factor is characterized by peaks at *m/z* 53 and 82 (Figure 4a). As discussed above, *m/z* 53 and 82 have been used as a tracer for SOA formed via IEPOX reactive uptake based on current knowledge. However, we cannot rule out the possibility that this factor also includes contribution from isoprene-OA formed via other pathways or the possibility that isoprene oxidation products other than IEPOX are taken up by acidic sulfate particles to generate *m/z* 53 and 82 [*Schwantes et al*., 2015]. Thus, we name the factor as isoprene-OA [*Xu et al*., 2015a; *Xu et al*., 2015b]. The time series of isoprene-OA correlates well with sulfate ($R = 0.73$), which is consistent with surface measurements in the southeastern United States [*Budisulistiorini et al*., 2016; *Budisulistiorini et al*., 2013; *Budisulistiorini et al*., 2015; *Xu et al*., 2015a; *Xu et al*., 2015b]. Isoprene-OA accounts for 24% of OA on average, with enhanced mass fraction in the Harllee Branch plume (Figure 4c).

Figure 5 shows the vertical profiles of the concentrations and mass fractions of OOA and isoprene-OA. The concentrations of both factors are relatively constant from the bottom of the profile to 2 km. Above 2 km, their concentrations decrease rapidly with altitude. At high altitude (i.e., >3 km), isoprene-OA concentration falls nearly to 0 and OOA dominates the OA (i.e., >90%). The vertical profile of isoprene-OA in this study is similar to the vertical profile of IEPOX sulfate ester over the southeastern United States [*Froyd et al*., 2010; *Liao et al*., 2015] and the vertical profile of isoprene SOA tracer ion *m/z* 82 over the Amazon [*Allan et al*., 2014] and Bornean rainforest [*Robinson et al*., 2011].

PMF analysis shows that the OA enhancement for the first two intercepts of Scherer plume is mainly due to an increase in OOA concentration. This OOA enhancement is likely caused by a biomass burning plume that partly merged with the Scherer plume (Figure S7). A biomass burning OA factor is not resolved from this flight, which is likely caused by the fact that the OA from biomass burning is aged and hence may be apportioned OOA factor by PMF analysis [*Grieshop et al*., 2009; *Hennigan et al*., 2011; *Xu et al*., 2015a]. It is also possible that the contribution from biomass burning OA to total OA is less than 5% so that PMF cannot retrieve the biomass burning OA factor [*Ulbrich et al*., 2009]. According to PMF analysis, isoprene-OA is the main

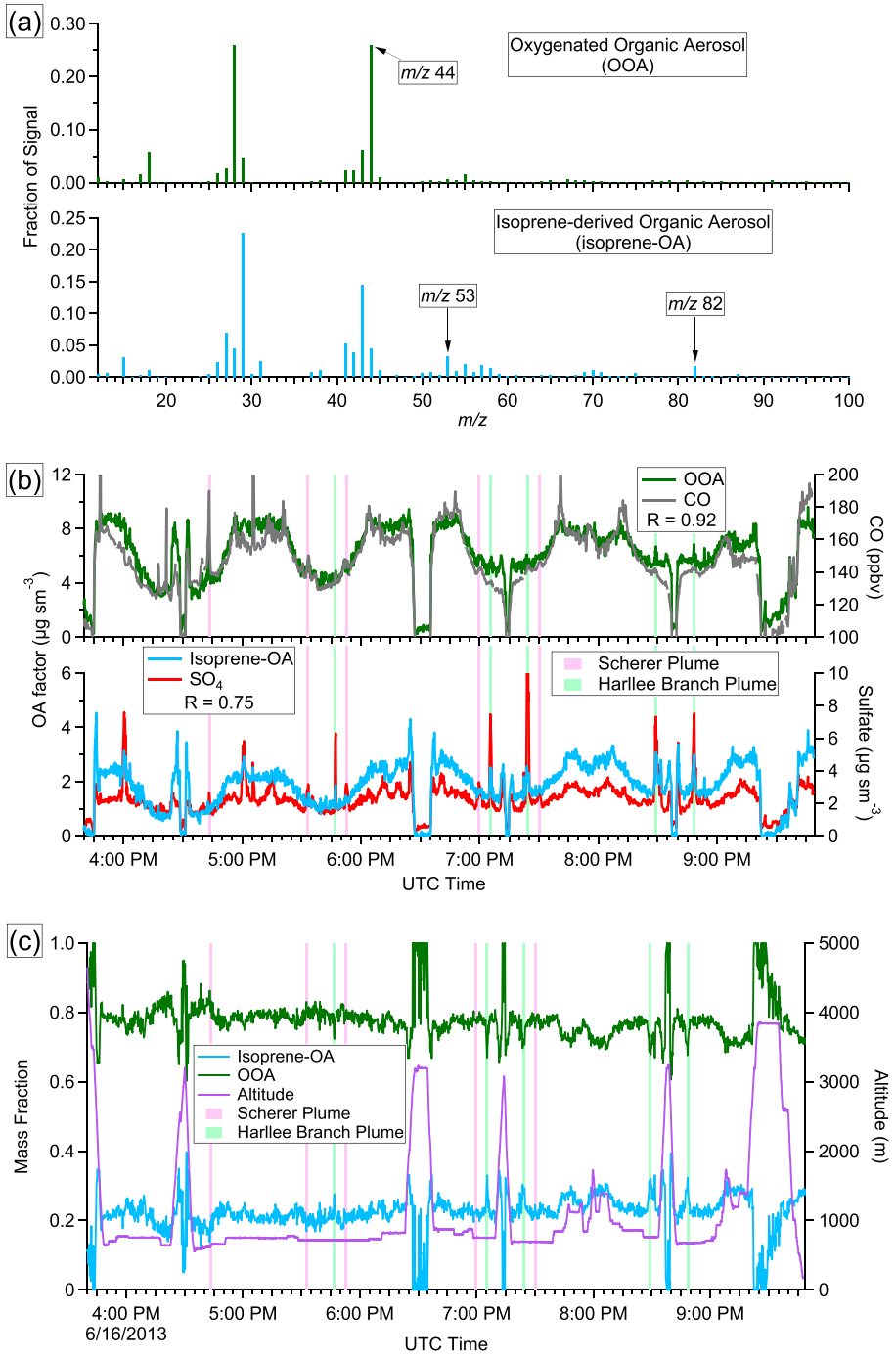

Figure 4. (a) Mass spectra, (b) time series, and (c) mass fractions of OA factors resolved from PMF analysis on the whole flight. The time series of corresponding external tracers are also shown in Figure 4b.

reason for the OA enhancement in the Harllee Branch plume. As shown in Figure 2e, isoprene-OA factor is substantially enhanced in the Harllee Branch plume, which is consistent with a large increase at signal *m/z* 82 inside the plume (Figure 3). In contrast, the isoprene-OA factor is not enhanced in the Scherer plume.

3.3. Reasons for Isoprene-OA Enhancement in Harllee Branch Plume

Next, we investigate the possible causes for the isoprene-OA enhancement in the Harllee Branch plume. Isoprene is depleted rapidly in the Harllee Branch plume [*de Gouw et al.*, 2015]. The gas phase chemistry in

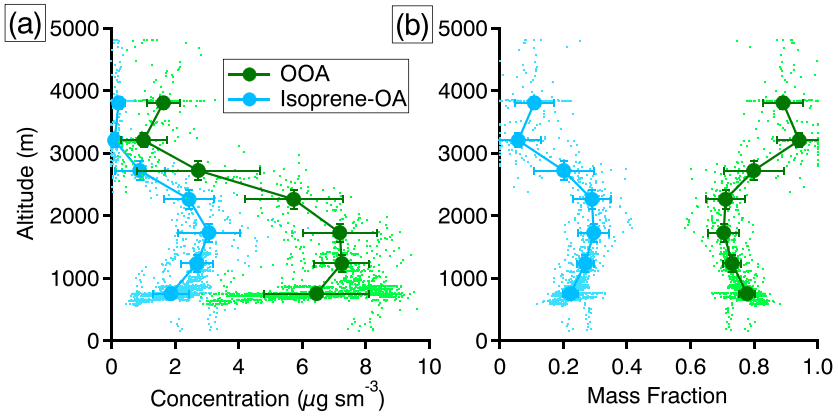

Figure 5. Vertical profile of (a) concentration and (b) mass fraction of OOA and isoprene-OA. The data are grouped based on 500 m increment in altitude. The error bars represent one standard deviation.

these plumes was investigated by *de Gouw et al.* [2015], who concluded that hydroxyl radical (OH) concentrations in both plumes were enhanced due to the presence of NO_x. The enhancements in OH concentration led to lower isoprene concentrations and increased concentration of isoprene products like formaldehyde in both plumes. Nevertheless, the oxidation of isoprene inside the Harllee Branch plume is unlikely to be the reason for the isoprene-OA enhancement. This is because of the high concentration of NO_x in the plume, which dominates the fate of RO_2 and inhibits the formation of IEPOX via the $RO_2 + HO_2$ pathway (supporting information). Similarly, the oxidation of ISOPOOH undergoes fragmentation and does not produce IEPOX in the plume [*St. Clair et al.*, 2016]. Although *Jacobs et al.* [2014] showed that the $RO_2 + NO$ pathway could also produce IEPOX, the IEPOX yield from that reaction is very small. For example, the largest reduction in isoprene observed in the third intercept of the Harllee Branch plume (i.e., ~1 ppb) would produce only 0.01 ppb IEPOX (~0.03 μg/m^3), which is too low to explain the magnitude of isoprene-OA enhancement. In addition, formaldehyde (HCHO), a product of isoprene oxidation via fragmentation [*Paulot et al.*, 2009a], is enhanced in the plume, which is likely due to enhanced OH concentration and NO dominating the fate of RO_2 in the plume [*de Gouw et al.*, 2015; *Wolfe et al.*, 2015]. Thus, based on current understanding on IEPOX formation mechanisms, it is unlikely that enhanced isoprene oxidation in the plume can produce enough IEPOX to explain the magnitude of isoprene-OA enhancement.

Background IEPOX, rather than IEPOX produced in the plume, likely dominated the isoprene-OA enhancement when it interacted with the sulfate-rich power plant plume. We perform a rough mass closure analysis to demonstrate that the reactive uptake of already existing IEPOX in the atmosphere could explain the isoprene-OA enhancement in the plume. Since IEPOX and ISOPOOH were measured as the same cluster ion at *m/z* 245 ($C_5H_{10}O_3I^-$) by I^- CIMS in this study, we apply a previously measured IEPOX/ISOPOOH concentration ratio to estimate IEPOX from the $C_5H_{10}O_3I^-$ signal using equation (2)

$$C_5H_{10}O_3I^- \text{ signal} = [\text{IEPOX}] \times \text{IEPOX sensitivity} + [\text{ISOPOOH}] \times \text{ISOPOOH sensitivity} \quad (2)$$

In equation (2), $C_5H_{10}O_3I^-$ signal (in unit of counts per second, cps) is measured by I^- CIMS in this study. The HR-CIMS sensitivities to IEPOX and ISOPOOH are 0.39 and 3.32 (cps ppt^{-1}), respectively. [IEPOX] and [ISOPOOH] are the concentration of IEPOX and ISOPOOH (ppt), respectively, which are to be determined. The IEPOX/ISOPOOH concentration ratio is estimated to be 1.04 ± 0.54 (average ± 1 standard deviation), based on the IEPOX and ISOPOOH measurements by a triple quadrupole CIMS during the Southeastern Oxidant and Aerosol Study (SOAS) and the Studies of Emissions and Atmospheric Composition, Clouds and Climate Coupling by Regional Surveys (SEAC4RS), which occurred over a similar region of the southeastern United States a few months after the SENEX project. After applying the estimated IEPOX/ISOPOOH concentration ratio to equation (2) and propagating uncertainties, we estimate that the IEPOX concentration is about 750 ± 546 ppt outside the Harllee Branch plume. Details about the estimation can be found in the supporting information. Then, assuming that all the IEPOX is taken up by the acidic particles in the plume and assuming a SOA yield of 20% from IEPOX reactive uptake [*Riedel et al.*, 2015], the IEPOX reactive uptake would produce

about $0.7 \pm 0.51\ \mu g\ sm^{-3}$ SOA, which is similar to the observed isoprene-OA enhancements in the plume (about $1\ \mu g\ sm^{-3}$ in Figure 2e). Despite large uncertainties in estimating IEPOX concentration, SOA yield, and IEPOX fate in the plume, this analysis demonstrates that the isoprene-OA enhancement in the plume could be explained by reactive uptake of IEPOX.

3.4. Parameterization of IEPOX Heterogeneous Reactions

To quantitatively support our argument that IEPOX reactive uptake process is fast and contributes to the OA enhancement in the Harllee Branch plume, we calculate the pseudo-first-order heterogeneous reaction rate constant for IEPOX reactive uptake (k_{het}, s^{-1}). The k_{het} can be calculated by following equation (3), neglecting the gas phase diffusion which has a minor effect on k_{het} [*Gaston et al.*, 2014].

$$k_{het} = \frac{\gamma v S_a}{4} \tag{3}$$

In equation (3), γ is the uptake coefficient of IEPOX, v is the mean molecular speed of IEPOX ($231\ m\ s^{-1}$ at 298 K), and S_a is the surface area of wet particles at ambient RH, which is calculated from the measured dry particle size distribution and κ-Köhler theory (supporting information). The parameter γ is parameterized based on a resistor model, which includes the mass accommodation at the surface (i.e., the first term in equation (4)) and aqueous-phase diffusion and reactions (i.e., the second term in equation (4)) [*Pye et al.*, 2013].

$$\frac{1}{\gamma} = \frac{1}{\alpha} + \frac{v}{4H_{IEPOX}RT\sqrt{D_a k_{aq}}} \frac{1}{f(q)} \tag{4}$$

$$f(q) = \coth(q) - \frac{1}{q} \tag{5}$$

$$q = r_p \sqrt{\frac{k_{aq}}{D_a}} \tag{6}$$

$$k_{aq} = \sum_{i=1}^{N} \sum_{j=1}^{M} k_{i,j} [\mathrm{nuc}_i]_{aq} [\mathrm{acid}_j]_{aq} \tag{7}$$

In equations (4)–(7), the mass accommodation coefficient, α, is estimated to be 0.1 by *Gaston et al.* [2014]; the diffusivity of IEPOX in the aqueous phase, D_a, is estimated to be $10^{-9}\ m^2\ s^{-1}$ by *Gharagheizi et al.* [2011]; r_p is the effective particle radius. The pseudo-first-order aqueous-phase rate constant, k_{aq}, is based on an acid-catalyzed ring-opening A-2 mechanism [*Eddingsaas et al.*, 2010]. $[nuc]_{aq}$ and $[acid]_{aq}$ represent the molarity ($mol\ L^{-1}$) of nucleophiles (SO_4^{2-} and H_2O) and acids (H^+ and HSO_4^-), respectively. The $k_{i,j}$ are the third-order rate constants for the reactions between IEPOX, acids (H^+ and HSO_4^-), and nucleophiles (SO_4^{2-} and H_2O). We applied the values of $k_{i,j}$ from *Riedel et al.* [2016], who estimated the $k_{i,j}$ values using a box model with experimental constraints. H_{IEPOX} is the Henry's Law coefficient of IEPOX. There are large uncertainties in many model parameters. For example, the H_{IEPOX}, which has been determined by model calculations and laboratory measurements, spans 2 orders of magnitude [*Chan et al.*, 2010; *Eddingsaas et al.*, 2010; *Gaston et al.*, 2014; *Nguyen et al.*, 2014; *Pye et al.*, 2013]. Here we apply the values of 3×10^7 and $1.7 \times 10^8\ M\ atm^{-1}$ based on measurements by *Nguyen et al.* [2014] and *Gaston et al.* [2014] for a sensitivity analysis. All the values of the parameters used in the calculation are summarized in Table S2. The parameterization is illustrated in Figure 6. The k_{aq} describes the IEPOX aqueous-phase reaction rate constant; γ evaluates the probability of gas particle collisions that leads to reaction; k_{het} describes the overall heterogeneous reaction rate constant of IEPOX, which includes two steps, IEPOX uptake to particles and subsequent aqueous-phase reactions.

In addition to the pseudo-first-order heterogeneous reaction rate constant for IEPOX reactive uptake (i.e., k_{het}), we also calculate the pseudo-first-order oxidation rate constant for IEPOX by OH radical (i.e., k_{ox}, s^{-1}). The k_{ox} is estimated by the product of OH concentration and the rate coefficient for the reaction of IEPOX and OH ($k_{OH+IEPOX}$) (equation (8)). The OH concentration in the power plant plumes is estimated by a Lagrangian plume dispersion model with photochemistry [*Brock et al.*, 2002; *Sillman*, 2000; *Wert et al.*, 2003]. There are two measured $k_{OH+IEPOX}$ values in the literature (i.e., 1.51×10^{-11} and

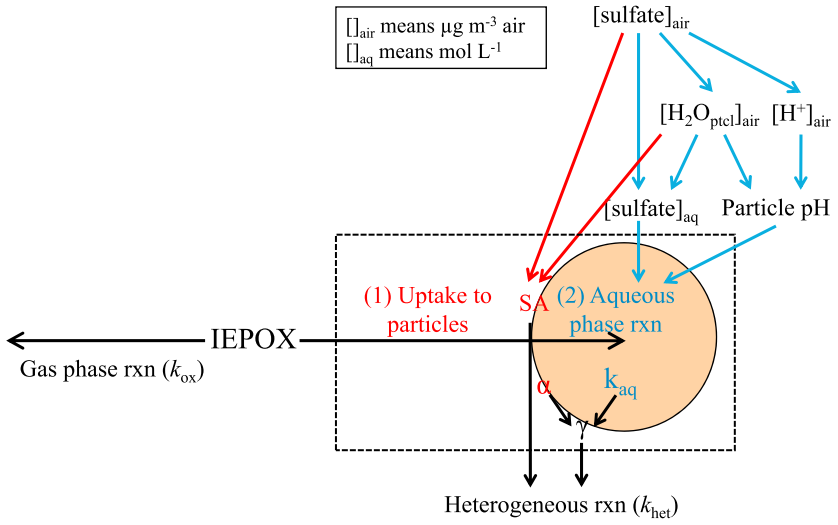

Figure 6. A schematic representation of the processes involved in the heterogeneous reaction of IEPOX and the effects of sulfate on the processes.

3.52×10^{-11} cm^3 molecule^{-1} s^{-1} at 298 K in *Bates et al.* [2014] and *Jacobs et al.* [2013], respectively), both of which are applied in this study for a sensitivity analysis.

$$k_{ox} = k_{IEPOX+OH}[OH] \quad (8)$$

Figure 7 shows the calculated k_{het} and k_{ox} for each intercept. In the Harllee Branch plume, the k_{het} is greater than 1.4×10^{-3} s^{-1}, which corresponds to an IEPOX lifetime shorter than 12 min (Figure S9), suggesting that the heterogeneous reaction is very fast. Also, the IEPOX heterogeneous reaction rate is 3–10 times faster than its gas phase oxidation rate, which indicates that the heterogeneous reaction is the major fate of IEPOX in the Harllee Branch plumes. Compared to Harllee Branch, the heterogeneous reaction rate is slower in Scherer, which is essentially caused by the smaller enhancement of sulfate in the Scherer plume. In Scherer, the IEPOX gas phase oxidation rate could be about half of its heterogeneous reaction rate (Figure 7), which implies that a portion of IEPOX may undergo OH oxidation, instead of heterogeneous reaction. This may explain the lack of isoprene-OA enhancement in Scherer.

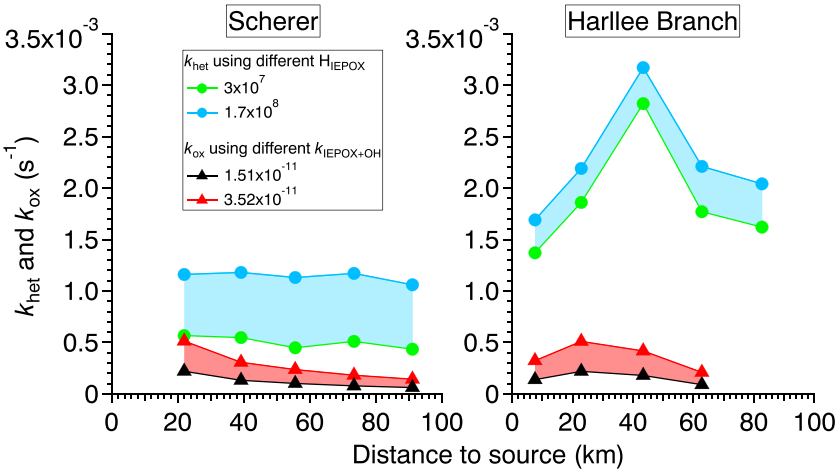

Figure 7. The pseudo-first-order reaction rate constants of IEPOX with respect to heterogeneous reaction and OH oxidation. Henry's law constants of IEPOX (H_{IEPOX}, in the unit of M atm^{-1}) are from *Nguyen et al.* [2014] and *Gaston et al.* [2014]. The rate coefficients for the reaction of IEPOX and OH ($k_{IEPOX+OH}$, in the unit of cm^3 molecule^{-1} s^{-1}) are from *Bates et al.* [2014] and *Jacobs et al.* [2013]. The lifetime of IEPOX with respect to heterogeneous reaction and OH oxidation are shown in Figure S9.

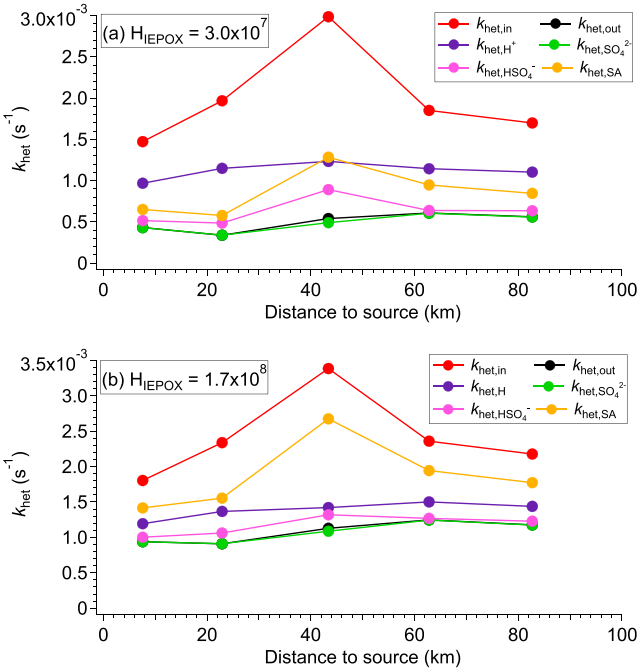

Figure 8. The pseudo-first-order heterogeneous reaction rate constant of IEPOX (k_{het}) inside and outside the plume. $k_{het,X}$ is calculated by using species concentrations outside the plume but only substituting the concentration of species X (X = H^+, SO_4^{2-}, HSO_4^-, and SA) with the value inside the plume. Different H_{IEPOX} values (M atm^{-1}) are used in Figures 8a and 8b.

3.5. Roles of Sulfate on Isoprene-OA Formation

The rapid heterogeneous reaction of IEPOX is a result of sulfate enhancements in the Harllee Branch plume, which is consistent with the finding that sulfate plays an important role in isoprene-OA formation in *Xu et al.* [2015b]. As shown in Figure 2b, the sulfate concentration is enhanced in the Harllee Branch plume by a factor of 2–5 compared to outside the plume, which is caused by the oxidation of SO_2. As a consequence of the sulfate enhancement, the particle acidity, particle water, and particle surface area in the plume are increased and correlated with each other (Figure 2). All these changes facilitate the IEPOX heterogeneous reaction. However, since these changes occur simultaneously, the separate effects (i.e., nucleophile versus acid catalyst versus uptake medium) are difficult to quantify. As shown in equation (3) and Figure 6, k_{het} is proportional to both surface area and γ (which is affected by particle acidity). The relative importance of surface area and particle acidity on k_{het} will be systematically assessed below.

First, we find that the nucleophilic effect of SO_4^{2-} is likely small. Although the absolute amount of SO_4^{2-} concentration in air (i.e., $[SO_4^{2-}]_{air}$, $[]_{air}$ indicates unit $\mu g\, m^{-3}$ air) increases in the plume (Figure S10e), its aqueous-phase concentration (i.e., $[SO_4^{2-}]_{aq}$, $[]_{aq}$ indicates unit $mol\, L^{-1}$) is not enhanced in the plume (Figure S10f). This is because for the same RH, higher $[SO_4^{2-}]_{air}$ leads to higher $[H_2O_{ptcl}]_{air}$, which dilutes the aqueous-phase SO_4^{2-} concentration and limits $[SO_4^{2-}]_{aq}$ enhancement. This suggests that the SO_4^{2-} nucleophilic effect is not likely the reason for the isoprene-OA enhancement in the plumes. We note that the $[SO_4^{2-}]_{aq}$ in the third Harllee Branch plume intercept is lower in the plume compared to outside. This is because the low particle pH in this intercept shifts the SO_4^{2-}-HSO_4^- equilibrium toward HSO_4^-, which results in lower $[SO_4^{2-}]_{aq}$ and higher $[HSO_4^-]_{aq}$ (Figure S10).

Particle acidity (i.e., $[H^+]_{aq}$) could affect k_{het} by influencing the IEPOX aqueous-phase reactions (k_{aq}) and hence γ (equations (7) and (4), respectively). In order to test the magnitude of this effect in the Harllee Branch plume, we first calculate k_{het} by using all the species concentration outside the plume (denoted as $k_{het,out}$) and k_{het} by using all the species concentration inside the plume (denoted as $k_{het,in}$). We then calculate a new k_{het} by using all the species concentration outside the plume but replacing only $[H^+]_{aq}$ with the concentration inside the plume (denoted as $k_{het,H+}$). By comparing the values of these different k_{het}, we can evaluate the effect of changing particle acidity alone on k_{het}. Figure 8 shows that $k_{het,H+}$ is larger than $k_{het,out}$, suggesting that increasing particle acidity contributes to k_{het} enhancement in the Harllee Branch plume. However, $k_{het,H+}$ accounts for 28–52% or 13–32% of k_{het} enhancement (i.e., calculated as $(k_{het,H+} - k_{het,out})/(k_{het,in} - k_{het,out})$), using an H_{IEPOX} value of 3.0×10^7 or 1.7×10^8 M atm^{-1}, respectively. This suggests that increasing particle acidity alone does not fully explain the enhanced magnitude of k_{het} in the plume according to the model.

Enhanced particle surface area also contributes to enhanced k_{het} in the Harllee Branch plume. Unlike particle acidity which affects k_{het} by influencing aqueous-phase reactions, particle surface area affects k_{het} by influencing the gas particle collision frequency and hence the amount of IEPOX uptake to particles. Figure 8 shows that $k_{het,SA}$ (calculated in a similar way as $k_{het,H+}$ discussed above) accounts for 15–30% or 45–69% of k_{het}

Table 1. The Effects of Increasing H^+ ($\mu g\,m^{-3}$), Particle Water ($\mu g\,m^{-3}$), or Sulfate ($\mu g\,m^{-3}$) on k_{het} While Holding the Other Covariates Constant

Increase in	Resulting Changes	Uptake to Particles	Aqueous-Phase Reaction	Overall Effect on k_{het}
$[Sulfate]_{air}$	$[H^+]_{aq}$ increases; surface area increases	increase	increase	always increase
$[H^+]_{air}$	$[H^+]_{aq}$ increases	no change	increase	may be small when k_{aq} is sufficiently large
$[H_2O_{ptcl}]_{air}$	$[H^+]_{aq}$ and $[SO_4^{2-}]_{aq}$ decrease; surface area increases	increase	decrease	may offset

enhancement using an H_{IEPOX} value of 3.0×10^7 or $1.7\times10^8\,M\,atm^{-1}$, implying that increasing particle surface area alone could possibly explain a large fraction of enhanced k_{het} in the plume.

Despite the uncertainties in H_{IEPOX}, it is clear that sulfate enhances isoprene-OA formation in the Harllee Branch plume due to both enhanced particle surface area (i.e., IEPOX uptake to particles) and particle acidity (i.e., aqueous-phase reactions).

3.6. Insights Into the Relationships Between Isoprene-OA, Sulfate, Particle Acidity, and Water

Xu et al. [2015b] observed a strong association between isoprene-OA and sulfate but a lack of correlation between isoprene-OA and particle water and acidity. Other studies have reported similar relationships [*Budisulistiorini et al*., 2015; *Lin et al*., 2013; *Rattanavaraha et al*., 2016; *Worton et al*., 2013]. The reason for these observations may arise from the competition between IEPOX uptake to particles and subsequent aqueous-phase reactions (summarized in Table 1 and Figure 6). Regarding the sulfate, its increase will not only enhance the aqueous-phase reaction but also enhance IEPOX uptake rate to particles as the case in Harllee Branch. Therefore, the overall IEPOX heterogeneous reaction rate is enhanced and the correlation between isoprene-OA and sulfate is expected. Although both particle acidity and particle water play an important role in the isoprene-OA formation, changes in particle acidity or particle water while other factors are held constant may only affect one aspect of k_{het} or have trade-off effects on k_{het}.

Increasing particle acidity will increase the aqueous-phase reaction rate constant (i.e., k_{aq}) and hence γ. Laboratory studies by *Gaston et al*. [2014] showed that particle acidity has the strongest effect on γ. It is important to note that γ only evaluates the probability of gas particle collisions that lead to reaction, but the IEPOX heterogeneous reaction lifetime (i.e., $1/k_{het}$) and isoprene-OA concentration depend not only on γ but also on the particle surface area (equation (3)). If the aqueous-phase reaction is sufficiently fast, γ saturates at the mass accommodation coefficient and the overall heterogeneous rate constant (i.e., k_{het}) is limited by particle surface area. Thus, increasing particle acidity may not increase the amount of isoprene-OA.

The observed lack of correlation between $[H_2O_{ptcl}]_{air}$ and isoprene-OA, even when other covariates are held constant, may be due to the trade-off effects of particle water on k_{het}. Higher $[H_2O_{ptcl}]_{air}$ increases particle surface area to potentially enhance IEPOX uptake. However, higher $[H_2O_{ptcl}]_{air}$ also dilutes the aqueous-phase concentration of compounds (i.e., $[H^+]_{aq}$, $[SO_4^{2-}]_{aq}$, $[HSO_4^-]_{aq}$), which decreases the aqueous-phase reaction rate constant (i.e., k_{aq}). To quantitatively evaluate the effects of particle water, we calculate the k_{het} by only changing $[H_2O_{ptcl}]_{air}$ and holding other covariates constant and similar to values measured at the Centreville, Alabama, during SOAS (supporting information). As shown in Figure 9, increasing $[H_2O_{ptcl}]_{air}$ dilutes particle phase concentrations which decreases γ, consistent with laboratory studies by *Nguyen et al*. [2014] and *Gaston et al*. [2014]. We note that the effect of $[H_2O_{ptcl}]_{air}$ on k_{het} is affected by H_{IEPOX} value. The k_{het} is insensitive to change in $[H_2O_{ptcl}]_{air}$ if an H_{IEPOX} value of $3.0\times10^7\,M\,atm^{-1}$ is used, which is due to the increase in surface area compensating the decrease in γ; however, k_{het} increases with $[H_2O_{ptcl}]_{air}$ if an H_{IEPOX} value of $1.7\times10^8\,M\,atm^{-1}$ is used. Nevertheless, this analysis quantitatively shows that the opposing effects of particle water could potentially explain the lack of association between $[H_2O_{ptcl}]_{air}$ and isoprene-OA. Regarding the role of particle water on SOA formation, *Carlton and Turpin* [2013] used a photochemical transport model and showed that the particle water largely controls the partitioning of water-soluble gas and subsequent SOA formation by providing partitioning medium in the southeastern U.S. However, since the dilution effect was not considered in *Carlton and Turpin* [2013], the role of particle water may be overestimated.

These competing effects may explain the observed relationships between isoprene-OA and different factors in previous studies. We note that the parameter values in the IEPOX heterogeneous reaction

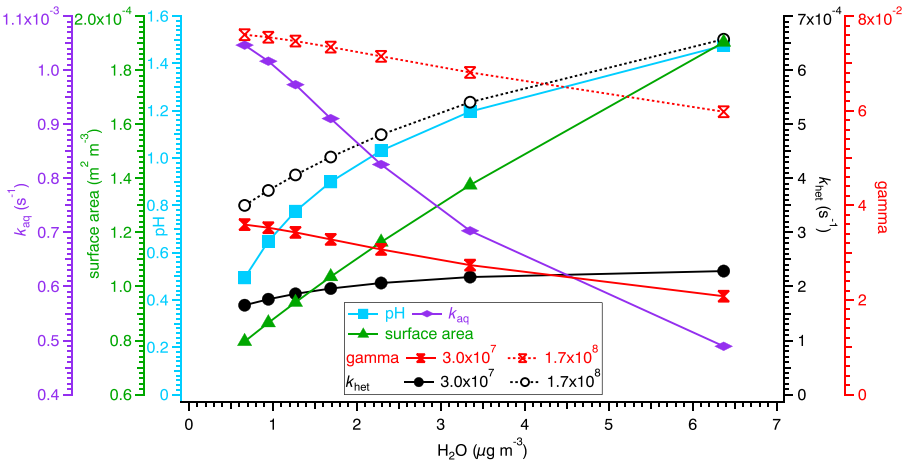

Figure 9. The effect of H_2O_{ptcl} ($\mu g\ m^{-3}$) on particle pH, k_{aq}, γ, surface area, and k_{het} while holding the other covariates (sulfate and H^+) constant. Different H_{IEPOX} values (3.0×10^7 and 1.7×10^8 in the unit of M atm^{-1}) are used.

parameterization are uncertain (such as α, H_{IEPOX}, and $k_{i,j}$'s in equations (4)–(7)), which highly limits quantitative understanding of the role of each factor. Further studies that constrain these parameters will improve predictions of isoprene-OA. In addition to the uncertainties of parameter values, one aspect that is missing in current IEPOX heterogeneous reaction parameterization is particle microphysical properties such as mixing state and particle morphology. Recent studies showed that the preexisting organic coatings may reduce the IEPOX heterogeneous reaction [*Gaston et al.*, 2014; *Riva et al.*, 2016]. Even if the particle composition is homogeneous, particles with the same sulfate mass concentration but different sulfate mass fraction may still result in different IEPOX heterogeneous rate. For example, particles with lower sulfate mass fraction would have less sulfate and fewer active sites for IEPOX uptake at the particle surface. This may inhibit IEPOX uptake to particles due to lower catalytic and nucleophilic activity of organics. Because less SO_2 was emitted by the Scherer plant, the resulting sulfate/organics ratio is 0.32–0.47 in Scherer plume, which is much lower than 0.65–1.21 in Harllee Branch plume. The newly formed sulfate in the Scherer plume mainly condensed onto preexisting particles, as suggested by the very small enhancement in particle number concentration (Figure S6f). Size distributions indicate that the number concentration of particles larger than 100 nm did not change in the Scherer plume, yet the volume concentration increased slightly, which is consistent with condensation of sulfate onto preexisting particles. Considering the high RH (>60%) in the atmosphere, the mixing time is likely short [*Song et al.*, 2015] so that the newly formed sulfate would be likely internally mixed with existing particles. In the Harllee Branch plume, there is a large enhancement in particle number concentration (Figure S6f), suggesting new particle formation from SO_2 oxidation. Furthermore, both the number and volume concentrations of particles larger than 100 nm increased in the Harllee Branch plume, indicating that some of the freshly formed sulfate particles remained separate from the preexisting population. Overall, there is more available sulfate and more active sites for IEPOX uptake in Harllee Branch plume. Therefore, in addition to the varying sulfate mass concentration, particle microphysical properties may also contribute to the difference in isoprene-OA enhancement between the two power plants. These results show that the effect of particle microphysical properties may be important and warrants future investigation.

4. Implications

Although the rapid reactive uptake of IEPOX to acidic particles has been observed in laboratory studies [*Gaston et al.*, 2014; *Liu et al.*, 2015; *Surratt et al.*, 2010], we report, for the first time, the rapid isoprene-OA formation via the IEPOX reactive uptake based on ambient measurements. We show that the sulfate, which is an oxidation product of SO_2 emitted from power plants, can enhance IEPOX uptake and facilitate the subsequent SOA formation, because sulfate enhances both IEPOX uptake to particles (i.e., through particle surface area) and aqueous-phase reactions (i.e., through particle acidity).

Airborne measurements of power plant plumes provide an opportunity to elucidate the magnitude of sulfate influence on isoprene-OA formation. As the isoprene-OA was formed rapidly in the plumes that were sampled

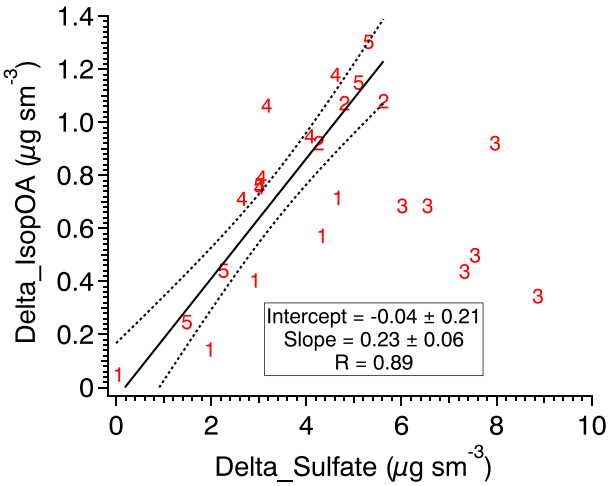

Figure 10. Scatterplot of the isoprene-OA enhancement (delta_isopOA) and the sulfate enhancement (delta_SO_4) in the Harllee Branch plume. The "delta" = concentration inside the plume − the average concentration of before and after the plume. The data points are labeled by the intercept number of Harllee Branch plume. The Intercept and slope are obtained by the orthogonal distance regression. The Pearson's *R* is from the linear least squares fitting. The dashed lines represent the 95% confidence level of orthogonal distance regression. The data from the third transect of Harllee Branch plume are not included in the fitting. The reason that the third transect of Harllee Branch plume does not follow the linear trend is not clear but may be due to differing background IEPOX concentration and/or enhanced OH concentration compared to other transects.

shortly after emission, we avoid challenges encountered in the interpretation of surface measurements, such as long-range transport and chemical aging of aerosol. For the Harllee Branch plume, we find that 1 μg sm^{-3} decrease in sulfate is associated with 0.23 ± 0.08 μg sm^{-3} decrease in isoprene-OA (Figure 10). The uncertainty is estimated by propagating the uncertainties of the linear correlation (26%), AMS measurement on this flight (18%), and isoprene-OA concentration from PMF analysis (13% by bootstrapping runs [*Ulbrich et al.*, 2009]). The magnitude of the sulfate effect on isoprene-OA formation observed here is consistent with *Blanchard et al.* [2015], who estimated that the future decrease in sulfate concentration by 1 μg m^{-3} would reduce OA concentration by 0.2 to 0.35 μg m^{-3} (assuming OA/OC = 1.4) based on statistical analysis on 14 years of data collected at multiple sites in the southeastern United States. The magnitude in our study is also similar to *Xu et al.* [2015b], who reported that 1 μg m^{-3} decrease in sulfate would lead to 0.42 μg m^{-3} reduction of isoprene-OA at the ground site of the SOAS. However, it is important to note that the magnitude of sulfate control on isoprene-OA reported in this study (i.e., 0.23 μg sm^{-3}) depends on the OH level. Plume OH is enhanced and reacts with IEPOX, which competes with IEPOX heterogeneous reaction. For example, while the sulfate concentration is enhanced in the Scherer plume (though weaker than Harllee Branch), the isoprene-OA is not enhanced, which is likely due to gas phase OH oxidation of IEPOX competing with IEPOX heterogeneous reaction.

The contrast in isoprene-OA concentration evolution between Harllee Branch (representative of older, inefficient, high NO_x and SO_2 emitting coal plants) and Scherer (representative of modern, more efficient, lower NO_x and SO_2 emitting coal plants) shows one benefit to air quality by implementing the emission control system and subsequent reducing SO_2 emission. This benefit should be considered in the perspective of the environmental impacts of electric power generation [*de Gouw et al.*, 2014]. *Hidy et al.* [2014] showed that sulfate concentration in the southeastern United States has reduced by ~3 μg m^{-3} (average of all SEARCH sites) in summer during the past 15 years. This sulfate reduction could cause ~0.7 μg m^{-3} reduction in OA by applying the magnitude of sulfate effect on isoprene-OA obtained from this study. Considering that OA decreases by 2.8 μg m^{-3} (average of all SEARCH sites and assuming OA/OC ratio of 1.4) [*Hidy et al.*, 2014], ~25% of the OA reduction could arise from the sulfate control over isoprene-OA formation. However, this estimation serves as an upper bound because the IEPOX concentration is expected to be lower in the past than the present, considering that ambient NO_x levels were substantially higher in the past and likely dominated the fate of RO_2. In the future, as the NO_x concentration is expected to keep decreasing due to emission regulations [*Pye et al.*, 2015], the formation of IEPOX would be enhanced and could potentially increase the importance of sulfate in terms of mediating isoprene-OA formation during the summer.

Acknowledgments

We are thankful for the staff at the NOAA Aircraft Operations Center and the WP-3D flight crew for help in instrumenting the aircraft and for conducting the flights. Georgia Tech researchers were supported by National Science Foundation (NSF) grant 1242258. N.L. Ng acknowledges U.S. Environmental Protection Agency STAR grant RD-83540301. A. Nenes acknowledges U.S. Environmental Protection Agency (EPA) STAR grant R835410. This publication's contents are solely the responsibility of the grantee and do not necessarily represent the official views of the U.S. EPA. Further, U.S. EPA does not endorse the purchase of any commercial products or services mentioned in the publication. The authors would like to thank Roya Bahreini, Thomas F. Hanisco, and Glenn M. Wolfe for helpful discussions. We thank Jason M. St. Clair, John D. Crounse, Alex P. Teng, Tran B. Nguyen, and Paul O. Wennberg for the triple quadrupole CIMS data. We thank the Kymberlee Osborne and Stefan France for synthesizing the authentic IEPOX. Data from the SENEX study are publicly available at http://www.esrl.noaa.gov/csd/projects/senex/. The research data beyond the SENEX campaign can be accessed upon request to the corresponding author.

References

Allan, J. D., W. T. Morgan, E. Darbyshire, M. J. Flynn, P. I. Williams, D. E. Oram, P. Artaxo, J. Brito, J. D. Lee, and H. Coe (2014), Airborne observations of IEPOX-derived isoprene SOA in the Amazon during SAMBBA, *Atmos. Chem. Phys.*, *14*(20), 11,393–11,407.

Bahreini, R., E. J. Dunlea, B. M. Matthew, C. Simons, K. S. Docherty, P. F. DeCarlo, J. L. Jimenez, C. A. Brock, and A. M. Middlebrook (2008), Design and operation of a pressure-controlled inlet for airborne sampling with an aerodynamic aerosol lens, *Aerosol Sci. Technol.*, *42*(6), 465–471.

Bahreini, R., et al. (2009), Organic aerosol formation in urban and industrial plumes near Houston and Dallas, Texas, *J. Geophys. Res.*, *114*, D00F16, doi:10.1029/2008011493.
Bates, K. H., J. D. Crounse, J. M. S. Clair, N. B. Bennett, T. B. Nguyen, J. H. Seinfeld, B. M. Stoltz, and P. O. Wennberg (2014), Gas phase production and loss of isoprene epoxydiols, *J. Phys. Chem. A*, *118*(7), 1237–1246.
Blanchard, C. L., G. M. Hidy, S. Shaw, K. Baumann, and E. S. Edgerton (2015), Effects of emission reductions on organic aerosol in the southeastern United States, *Atmos. Chem. Phys. Discuss.*, *15*(12), 17,051–17,092.
Brock, C. A., et al. (2002), Particle growth in the plumes of coal-fired power plants, *J. Geophys. Res.*, *107*(D12), 4155, doi:10.1029/2001JD001062.
Brock, C. A., et al. (2016), Aerosol optical properties in the southeastern United States in summer – Part 1: Hygroscopic growth, *Atmos. Chem. Phys.*, *16*(8), 4987–5007.
Budisulistiorini, S. H., et al. (2013), Real-time continuous characterization of secondary organic aerosol derived from isoprene epoxydiols in downtown Atlanta, Georgia, using the Aerodyne Aerosol Chemical Speciation Monitor, *Environ. Sci. Technol.*, *47*(11), 5686–5694.
Budisulistiorini, S. H., et al. (2015), Examining the effects of anthropogenic emissions on isoprene-derived secondary organic aerosol formation during the 2013 Southern Oxidant and Aerosol Study (SOAS) at the Look Rock, Tennessee ground site, *Atmos. Chem. Phys.*, *15*(15), 8871–8888.
Budisulistiorini, S. H., K. Baumann, E. S. Edgerton, S. T. Bairai, S. Mueller, S. L. Shaw, E. M. Knipping, A. Gold, and J. D. Surratt (2016), Seasonal characterization of submicron aerosol chemical composition and organic aerosol sources in the southeastern United States: Atlanta, Georgia,and Look Rock, Tennessee, *Atmos. Chem. Phys.*, *16*(8), 5171–5189.
Canagaratna, M. R., et al. (2007), Chemical and microphysical characterization of ambient aerosols with the aerodyne aerosol mass spectrometer, *Mass Spectrom. Rev.*, *26*(2), 185–222.
Canagaratna, M. R., et al. (2015), Elemental ratio measurements of organic compounds using aerosol mass spectrometry: Characterization, improved calibration, and implications, *Atmos. Chem. Phys.*, *15*(1), 253–272.
Carlton, A. G., and B. J. Turpin (2013), Particle partitioning potential of organic compounds is highest in the Eastern US and driven by anthropogenic water, *Atmos. Chem. Phys.*, *13*(20), 10,203–10,214.
Carlton, A. G., R. W. Pinder, P. V. Bhave, and G. A. Pouliot (2010), To what extent can biogenic SOA be controlled? *Environ. Sci. Technol.*, *44*(9), 3376–3380.
Cerully, K. M., A. Bougiatioti, J. R. Hite Jr., H. Guo, L. Xu, N. L. Ng, R. Weber, and A. Nenes (2015), On the link between hygroscopicity, volatility, and oxidation state of ambient and water-soluble aerosols in the southeastern United States, *Atmos. Chem. Phys.*, *15*(15), 8679–8694.
Chan, M. N., et al. (2010), Characterization and quantification of isoprene-derived epoxydiols in ambient aerosol in the southeastern United States, *Environ. Sci. Technol.*, *44*(12), 4590–4596.
Chen, Q., et al. (2015), Submicron particle mass concentrations and sources in the Amazonian wet season (AMAZE-08), *Atmos. Chem. Phys.*, *15*(7), 3687–3701.
de Gouw, J. A., D. D. Parrish, G. J. Frost, and M. Trainer (2014), Reduced emissions of CO_2, NO_x, and SO_2 from U.S. power plants owing to switch from coal to natural gas with combined cycle technology, *Earth's Future*, *2*(2), 75–82.
de Gouw, J. A., et al. (2015), Enhanced removal of biogenic hydrocarbons in power plant plumes constrains the dependence of atmospheric hydroxyl concentrations on nitrogen oxides, Abstract A13G-08 presented at 2015 Fall Meeting, AGU, San Francisco, Calif., 14–18 Dec.
Eddingsaas, N. C., D. G. VanderVelde, and P. O. Wennberg (2010), Kinetics and products of the acid-catalyzed ring-opening of atmospherically relevant butyl epoxy alcohols, *J. Phys. Chem. A*, *114*(31), 8106–8113.
Edney, E. O., T. E. Kleindienst, M. Jaoui, M. Lewandowski, J. H. Offenberg, W. Wang, and M. Claeys (2005), Formation of 2-methyl tetrols and 2-methylglyceric acid in secondary organic aerosol from laboratory irradiated isoprene/NO_x/SO_2/air mixtures and their detection in ambient $PM_{2.5}$ samples collected in the eastern United States, *Atmos. Environ.*, *39*(29), 5281–5289.
Fountoukis, C., and A. Nenes (2007), ISORROPIA II: A computationally efficient thermodynamic equilibrium model for K^+-Ca^{2+}-Mg^{2+}-NH_4^+-Na^+-SO_4^{2-}-NO_3^--Cl^--H_2O aerosols, *Atmos. Chem. Phys.*, *7*(17), 4639–4659.
Froyd, K. D., S. M. Murphy, D. M. Murphy, J. A. de Gouw, N. C. Eddingsaas, and P. O. Wennberg (2010), Contribution of isoprene-derived organosulfates to free tropospheric aerosol mass, *Proc. Natl. Acad. Sci. U.S.A.*, *107*(50), 21,360–21,365.
Gaston, C. J., T. P. Riedel, Z. Zhang, A. Gold, J. D. Surratt, and J. A. Thornton (2014), Reactive uptake of an isoprene-derived epoxydiol to submicron aerosol particles, *Environ. Sci. Technol.*, *48*(19), 11,178–11,186.
Gharagheizi, F., A. Eslamimanesh, A. H. Mohammadi, and D. Richon (2011), Representation and prediction of molecular diffusivity of nonelectrolyte organic compounds in water at infinite dilution using the artificial neural network-group contribution method, *J. Chem. Eng. Data*, *56*(5), 1741–1750.
Goldstein, A. H., C. D. Koven, C. L. Heald, and I. Y. Fung (2009), Biogenic carbon and anthropogenic pollutants combine to form a cooling haze over the southeastern United States, *Proc. Natl. Acad. Sci. U.S.A.*, *106*(22), 8835–8840.
Grieshop, A. P., N. M. Donahue, and A. L. Robinson (2009), Laboratory investigation of photochemical oxidation of organic aerosol from wood fires 2: Analysis of aerosol mass spectrometer data, *Atmos. Chem. Phys.*, *9*(6), 2227–2240.
Guenther, A., X. Jiang, C. L. Heald, T. Sakulyanontvittaya, T. Duhl, L. K. Emmons, and X. Wang (2012), The Model of Emissions of Gases and Aerosols from Nature version 2.1 (MEGAN2.1): An extended and updated framework for modeling biogenic emissions, *Geosci. Model Dev.*, *5*(6), 1471–1492.
Guo, H., et al. (2015), Fine-particle water and pH in the southeastern United States, *Atmos. Chem. Phys.*, *15*(9), 5211–5228.
Hallquist, M., et al. (2009), The formation, properties and impact of secondary organic aerosol: Current and emerging issues, *Atmos. Chem. Phys.*, *9*(14), 5155–5236.
Hennigan, C. J., et al. (2011), Chemical and physical transformations of organic aerosol from the photo-oxidation of open biomass burning emissions in an environmental chamber, *Atmos. Chem. Phys.*, *11*(15), 7669–7686.
Hennigan, C. J., J. Izumi, A. P. Sullivan, R. J. Weber, and A. Nenes (2015), A critical evaluation of proxy methods used to estimate the acidity of atmospheric particles, *Atmos. Chem. Phys.*, *15*(5), 2775–2790.
Hidy, G. M., C. L. Blanchard, K. Baumann, E. Edgerton, S. Tanenbaum, S. Shaw, E. Knipping, I. Tombach, J. Jansen, and J. Walters (2014), Chemical climatology of the southeastern United States, 1999–2013, *Atmos. Chem. Phys.*, *14*(21), 11,893–11,914.
Hoyle, C. R., et al. (2011), A review of the anthropogenic influence on biogenic secondary organic aerosol, *Atmos. Chem. Phys.*, *11*(1), 321–343.
Hu, W. W., et al. (2015), Characterization of a real-time tracer for isoprene epoxydiols-derived secondary organic aerosol (IEPOX-SOA) from aerosol mass spectrometer measurements, *Atmos. Chem. Phys.*, *15*(20), 11,807–11,833.
Jacobs, M. I., A. I. Darer, and M. J. Elrod (2013), Rate constants and products of the OH reaction with isoprene-derived epoxides, *Environ. Sci. Technol.*, *47*(22), 12,868–12,876.
Jacobs, M. I., W. J. Burke, and M. J. Elrod (2014), Kinetics of the reactions of isoprene-derived hydroxynitrates: Gas phase epoxide formation and solution phase hydrolysis, *Atmos. Chem. Phys.*, *14*(17), 8933–8946.

Jimenez, J. L., et al. (2009), Evolution of organic aerosols in the atmosphere, *Science*, *326*(5959), 1525–1529.
Kleindienst, T. E., E. O. Edney, M. Lewandowski, J. H. Offenberg, and M. Jaoui (2006), Secondary organic carbon and aerosol yields from the irradiations of isoprene and alpha-pinene in the presence of NO_x and SO_2, *Environ. Sci. Technol.*, *40*(12), 3807–3812.
Lee, B. H., F. D. Lopez-Hilfiker, C. Mohr, T. Kurtén, D. R. Worsnop, and J. A. Thornton (2014), An iodide-adduct high-resolution time-of-flight chemical-ionization mass spectrometer: Application to atmospheric inorganic and organic compounds, *Environ. Sci. Technol.*, *48*(11), 6309–6317.
Liao, H., D. K. Henze, J. H. Seinfeld, S. Wu, and L. J. Mickley (2007), Biogenic secondary organic aerosol over the United States: Comparison of climatological simulations with observations, *J. Geophys. Res.*, *112*, D06201, doi:10.1029/2006JD007813.
Liao, J., et al. (2015), Airborne measurements of organosulfates over the continental U.S., *J. Geophys. Res. Atmos.*, *120*, 2990–3005, doi:10.1002/2014JD022378.
Lin, Y. H., et al. (2012), Isoprene epoxydiols as precursors to secondary organic aerosol formation: Acid-catalyzed reactive uptake studies with authentic compounds, *Environ. Sci. Technol.*, *46*(1), 250–258.
Lin, Y. H., E. M. Knipping, E. S. Edgerton, S. L. Shaw, and J. D. Surratt (2013), Investigating the influences of SO_2 and NH_3 levels on isoprene-derived secondary organic aerosol formation using conditional sampling approaches, *Atmos. Chem. Phys.*, *13*(16), 8457–8470.
Liu, Y., M. Kuwata, B. F. Strick, F. M. Geiger, R. J. Thomson, K. A. McKinney, and S. T. Martin (2015), Uptake of epoxydiol isomers accounts for half of the particle-phase material produced from isoprene photooxidation via the HO_2 pathway, *Environ. Sci. Technol.*, *49*(1), 250–258.
Marais, E. A., et al. (2015), Aqueous-phase mechanism for secondary organic aerosol formation from isoprene: Application to the Southeast United States and co-benefit of SO_2 emission controls, *Atmos. Chem. Phys. Discuss.*, *15*(21), 32,005–32,047.
McNeill, V. F. (2015), Aqueous organic chemistry in the atmosphere: Sources and chemical processing of organic aerosols, *Environ. Sci. Technol.*, *49*(3), 1237–1244.
McNeill, V. F., J. L. Woo, D. D. Kim, A. N. Schwier, N. J. Wannell, A. J. Sumner, and J. M. Barakat (2012), Aqueous-phase secondary organic aerosol and organosulfate formation in atmospheric aerosols: A modeling study, *Environ. Sci. Technol.*, *46*(15), 8075–8081.
Middlebrook, A. M., R. Bahreini, J. L. Jimenez, and M. R. Canagaratna (2012), Evaluation of composition-dependent collection efficiencies for the aerodyne aerosol mass spectrometer using field data, *Aerosol Sci. Technol.*, *46*(3), 258–271.
Ng, N. L., et al. (2010), Organic aerosol components observed in Northern Hemispheric datasets from Aerosol Mass Spectrometry, *Atmos. Chem. Phys.*, *10*(10), 4625–4641.
Nguyen, T. B., M. M. Coggon, K. H. Bates, X. Zhang, R. H. Schwantes, K. A. Schilling, C. L. Loza, R. C. Flagan, P. O. Wennberg, and J. H. Seinfeld (2014), Organic aerosol formation from the reactive uptake of isoprene epoxydiols (IEPOX) onto non-acidified inorganic seeds, *Atmos. Chem. Phys.*, *14*(7), 3497–3510.
Paulot, F., J. D. Crounse, H. G. Kjaergaard, J. H. Kroll, J. H. Seinfeld, and P. O. Wennberg (2009a), Isoprene photooxidation: New insights into the production of acids and organic nitrates, *Atmos. Chem. Phys.*, *9*(4), 1479–1501.
Paulot, F., J. D. Crounse, H. G. Kjaergaard, A. Kurten, J. M. S. Clair, J. H. Seinfeld, and P. O. Wennberg (2009b), Unexpected epoxide formation in the gas-phase photooxidation of isoprene, *Science*, *325*(5941), 730–733.
Petters, M. D., and S. M. Kreidenweis (2007), A single parameter representation of hygroscopic growth and cloud condensation nucleus activity, *Atmos. Chem. Phys.*, *7*(8), 1961–1971.
Pye, H. O. T., et al. (2013), Epoxide pathways improve model predictions of isoprene markers and reveal key role of acidity in aerosol formation, *Environ. Sci. Technol.*, *47*(19), 11,056–11,064.
Pye, H. O. T., et al. (2015), Modeling the current and future roles of particulate organic nitrates in the southeastern United States, *Environ. Sci. Technol.*, *49*(24), 14,195–14,203.
Rattanavaraha, W., et al. (2016), Assessing the impact of anthropogenic pollution on isoprene-derived secondary organic aerosol formation in $PM_{2.5}$ collected from the Birmingham, Alabama, ground site during the 2013 Southern Oxidant and Aerosol Study, *Atmos. Chem. Phys.*, *16*(8), 4897–4914.
Riedel, T. P., Y.-H. Lin, S. H. Budisulistiorini, C. J. Gaston, J. A. Thornton, Z. Zhang, W. Vizuete, A. Gold, and J. D. Surratt (2015), Heterogeneous reactions of isoprene-derived epoxides: Reaction probabilities and molar secondary organic aerosol yield estimates, *Environ. Sci. Technol. Lett.*, *2*, 38–42.
Riedel, T. P., Y. H. Lin, Z. Zhang, K. Chu, J. A. Thornton, W. Vizuete, A. Gold, and J. D. Surratt (2016), Constraining condensed-phase formation kinetics of secondary organic aerosol components from isoprene epoxydiols, *Atmos. Chem. Phys.*, *16*(3), 1245–1254.
Riva, M., D. M. Bell, A.-M. K. Hansen, G. T. Drozd, Z. Zhang, A. Gold, D. Imre, J. D. Surratt, M. Glasius, and A. Zelenyuk (2016), Effect of organic coatings, humidity and aerosol acidity on multiphase chemistry of isoprene epoxydiols, *Environ. Sci. Technol.*, *50*, 5580–5588.
Robinson, N. H., et al. (2011), Evidence for a significant proportion of secondary organic aerosol from isoprene above a maritime tropical forest, *Atmos. Chem. Phys.*, *11*(3), 1039–1050.
Schwantes, R. H., A. P. Teng, T. B. Nguyen, M. M. Coggon, J. D. Crounse, J. M. S. Clair, X. Zhang, K. A. Schilling, J. H. Seinfeld, and P. O. Wennberg (2015), Isoprene NO_3 oxidation products from the $RO_2 + HO_2$ pathway, *J. Phys. Chem. A*, *119*, 10,158–10,171.
Sillman, S. (2000), Ozone production efficiency and loss of NO_x in power plant plumes: Photochemical model and interpretation of measurements in Tennessee, *J. Geophys. Res.*, *105*(D7), 9189–9202, doi:10.1029/1999JD901014.
Slowik, J. G., et al. (2011), Photochemical processing of organic aerosol at nearby continental sites: Contrast between urban plumes and regional aerosol, *Atmos. Chem. Phys.*, *11*(6), 2991–3006.
Song, M., P. F. Liu, S. J. Hanna, Y. J. Li, S. T. Martin, and A. K. Bertram (2015), Relative humidity-dependent viscosities of isoprene-derived secondary organic material and atmospheric implications for isoprene-dominant forests, *Atmos. Chem. Phys.*, *15*(9), 5145–5159.
Spracklen, D. V., et al. (2011), Aerosol mass spectrometer constraint on the global secondary organic aerosol budget, *Atmos. Chem. Phys.*, *11*(23), 12,109–12,136.
St. Clair, J. M., J. C. Rivera-Rios, J. D. Crounse, H. C. Knap, K. H. Bates, A. P. Teng, S. Jørgensen, H. G. Kjaergaard, F. N. Keutsch, and P. O. Wennberg (2016), Kinetics and products of the reaction of the first-generation isoprene hydroxy hydroperoxide (ISOPOOH) with OH, *J. Phys. Chem. A*, *120*(9), 1441–1451.
Sullivan, A. P., R. E. Peltier, C. A. Brock, J. A. de Gouw, J. S. Holloway, C. Warneke, A. G. Wollny, and R. J. Weber (2006), Airborne measurements of carbonaceous aerosol soluble in water over northeastern United States: Method development and an investigation into water-soluble organic carbon sources, *J. Geophys. Res.*, *111*, D23S46, doi:10.1029/2006JD007072.
Surratt, J. D., M. Lewandowski, J. H. Offenberg, M. Jaoui, T. E. Kleindienst, E. O. Edney, and J. H. Seinfeld (2007), Effect of acidity on secondary organic aerosol formation from isoprene, *Environ. Sci. Technol.*, *41*(15), 5363–5369.
Surratt, J. D., A. W. H. Chan, N. C. Eddingsaas, M. N. Chan, C. L. Loza, A. J. Kwan, S. P. Hersey, R. C. Flagan, P. O. Wennberg, and J. H. Seinfeld (2010), Reactive intermediates revealed in secondary organic aerosol formation from isoprene, *Proc. Natl. Acad. Sci. U.S.A.*, *107*(15), 6640–6645.

Ulbrich, I. M., M. R. Canagaratna, Q. Zhang, D. R. Worsnop, and J. L. Jimenez (2009), Interpretation of organic components from positive matrix factorization of aerosol mass spectrometric data, *Atmos. Chem. Phys.*, *9*(9), 2891–2918.

Wagner, N. L., et al. (2015), In situ vertical profiles of aerosol extinction, mass, and composition over the southeast United States during SENEX and SEAC4RS: Observations of a modest aerosol enhancement aloft, *Atmos. Chem. Phys.*, *15*(12), 7085–7102.

Wang, W., I. Kourtchev, B. Graham, J. Cafmeyer, W. Maenhaut, and M. Claeys (2005), Characterization of oxygenated derivatives of isoprene related to 2-methyltetrols in Amazonian aerosols using trimethylsilylation and gas chromatography/ion trap mass spectrometry, *Rapid Commun. Mass Spectrom.*, *19*(10), 1343–1351.

Warneke, C., et al. (2016), Instrumentation and measurement strategy for the NOAA SENEX aircraft campaign as part of the Southeast Atmosphere Study 2013, *Atmos. Meas. Tech. Discuss.*, *2016*, 1–39.

Weber, R. J., et al. (2007), A study of secondary organic aerosol formation in the anthropogenic-influenced southeastern United States, *J. Geophys. Res.*, *112*, D13302, doi:10.1029/2007JD008408.

Wert, B. P., et al. (2003), Signatures of terminal alkene oxidation in airborne formaldehyde measurements during TexAQS 2000, *J. Geophys. Res.*, *108*(D3), 4104, doi:10.1029/2002JD002502.

Wolfe, G. M., et al. (2015), Formaldehyde production from isoprene oxidation across NO_x regimes, *Atmos. Chem. Phys. Discuss.*, *15*(21), 31,587–31,620.

Worton, D. R., et al. (2011), Origins and composition of fine atmospheric carbonaceous aerosol in the Sierra Nevada Mountains, California, *Atmos. Chem. Phys.*, *11*(19), 10,219–10,241.

Worton, D. R., et al. (2013), Observational insights into aerosol formation from isoprene, *Environ. Sci. Technol.*, *47*(20), 11,403–11,413.

Xu, L., S. Suresh, H. Guo, R. J. Weber, and N. L. Ng (2015a), Aerosol characterization over the southeastern United States using high-resolution aerosol mass spectrometry: Spatial and seasonal variation of aerosol composition and sources with a focus on organic nitrates, *Atmos. Chem. Phys.*, *15*(13), 7307–7336.

Xu, L., et al. (2015b), Effects of anthropogenic emissions on aerosol formation from isoprene and monoterpenes in the southeastern United States, *Proc. Natl. Acad. Sci. U.S.A.*, *112*(1), 37–42.